Supporting Information

Triallyl cyanurate copolymerization delivered nonflammable and fast ion conduction elastic polymer electrolyte

*Dashan Zhang [ab], Yongzheng Shi [ab], Junwei An [cd], Shubin Yang [a], Bin Li *[ab]*

[a] School of Materials Science & Engineering, Beihang University, Beijing, China

[b] State Key Laboratory of Powder Metallurgy, Central South University, Changsha, China

[c] School of Chemistry and Chemical Engineering, Jining Normal University, No. 59 Gongnong Street, Wulanchabu City, Inner Mongolia Autonomous Region, China

[d] Inner Mongolia Qingmeng Graphene Technology Co., Ltd. China Graphite Application Industrial Park, Xingwangjiao Industrial Park, Xinghe County, Wulanchabu City, Inner Mongolia Autonomous Region, China

* Corresponding author:

E-mail addresses: li_bin@buaa.edu.cn

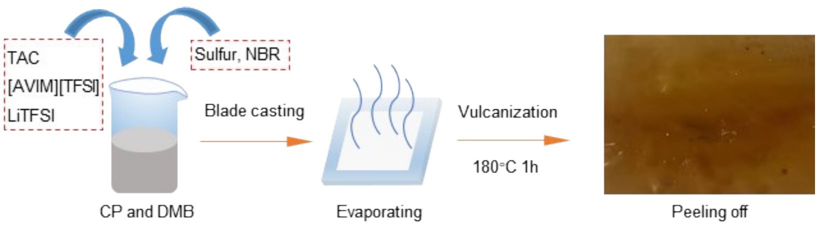

Figure S1. Schematic of synthetic processes of v-NBR/TAC/IL electrolyte membrane.

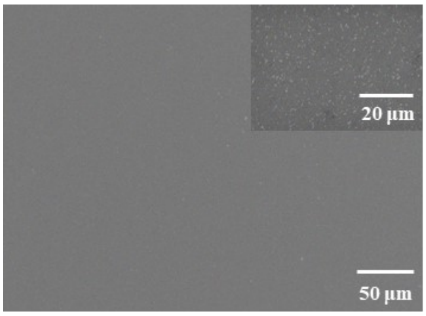

Figure S2. SEM image of the surface of v-NBR/TAC/IL electrolyte membrane.

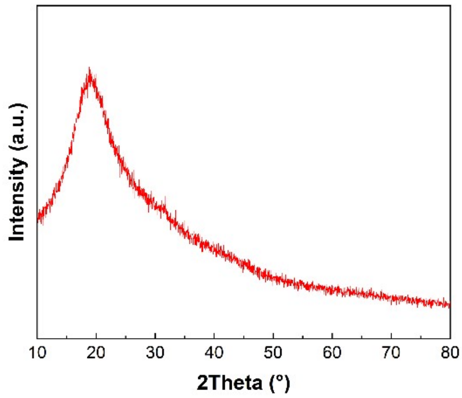

Figure S3. XRD spectra of v-NBR/TAC/IL electrolyte.

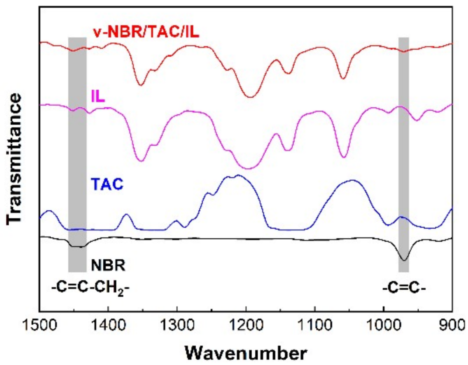

Figure S4. Enlarged Fourier Transform Infrared (FTIR) spectra of the NBR, TAC, IL and v-NBR/TAC/IL electrolyte.

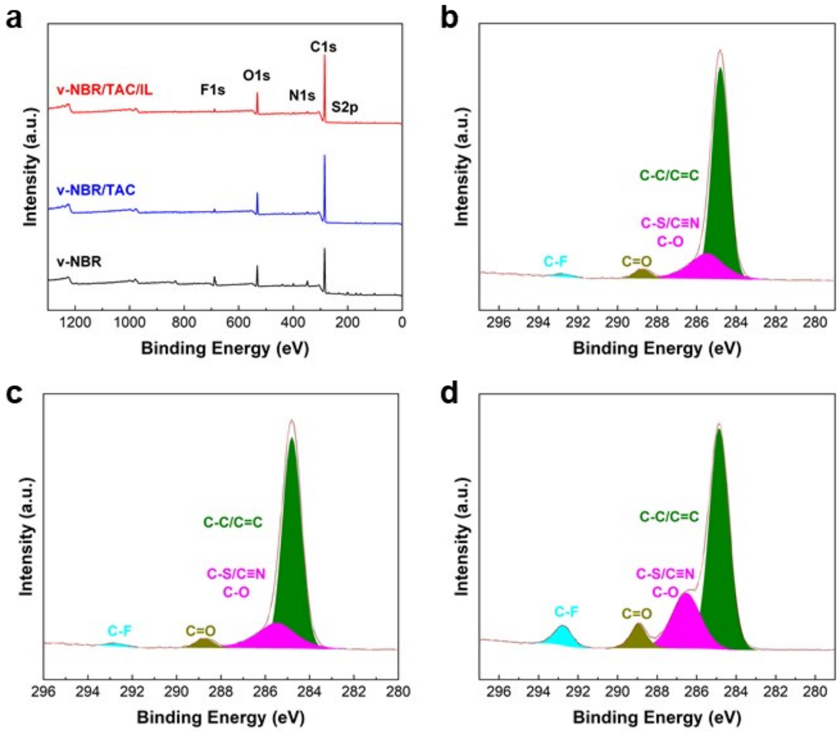

Figure S5. (a) XPS spectrum of SPEs. And comparation of C 1s spectrum among the (b) v-NBR electrolyte, (c) v-NBR/TAC electrolyte and (d) v-NBR/TAC/IL electrolyte.

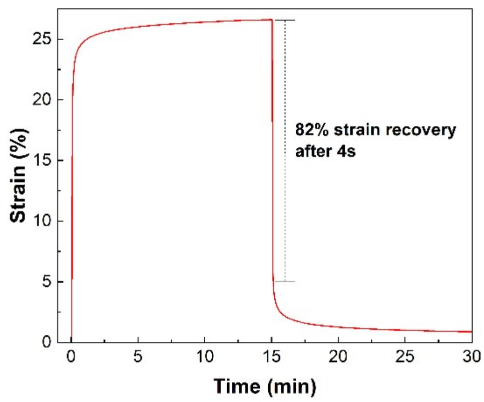

Figure S6. Creep test of v-NBR/TAC/IL electrolyte membrane.

The membrane can rapidly recover from large strains, demonstrating its high elasticity and resilience.

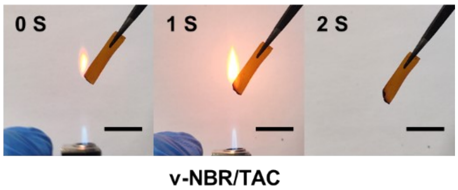

Figure S7. Flame tests of v-NBR/TAC electrolyte membrane. Scale bars, 1 cm.

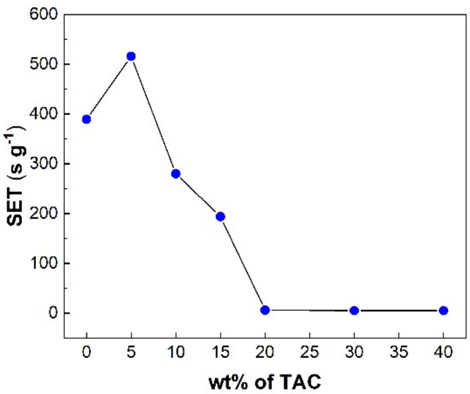

Figure S8. The SET of v-NBR/TAC electrolyte with different weight percentages of TAC.

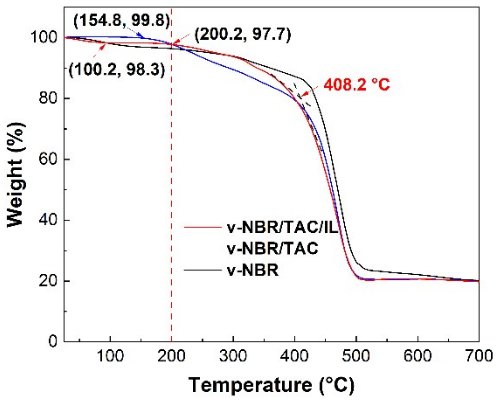

Figure S9. TGA thermograms of SPEs at N_2 atmosphere.

The v-NBR/TAC/IL electrolyte suffers only ~2.3 wt.% mass drop from room temperature to 200 ^{o}C, corresponding to the decomposition of a few small molecules in the electrolyte. Compared with v-NBR/TAC electrolyte and v-NBR electrolyte, it can be proved that v-NBR/TAC/IL electrolyte has high thermal stability.

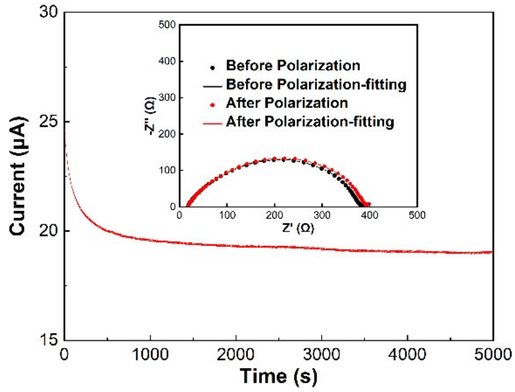

Figure S10. Lithium transference number measurements of v-NBR/TAC/IL electrolyte.

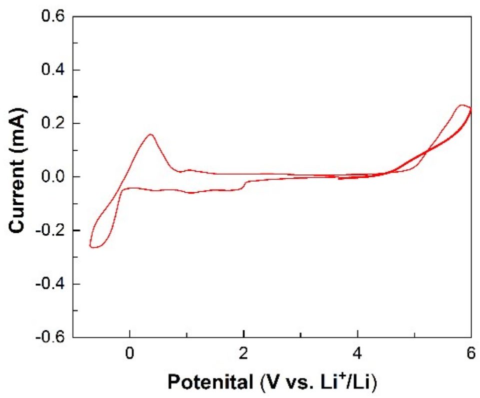

Figure S11. CV curves of Li|v-NBR/TAC/IL|ss.

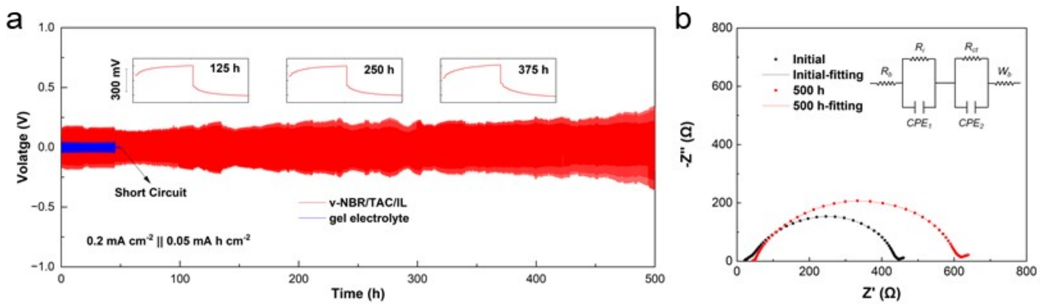

Figure S12. (a) Long-term cycling tests of Li plating/stripping for Li−Li symmetrical batteries with v-NBR/TAC/IL electrolyte and gel electrolyte at current densities of 0.2 mA cm^{-2} for 0.05 mAh cm^{-2} at room temperature. And (b) corresponding EIS plots with v-NBR/TAC/IL electrolyte.

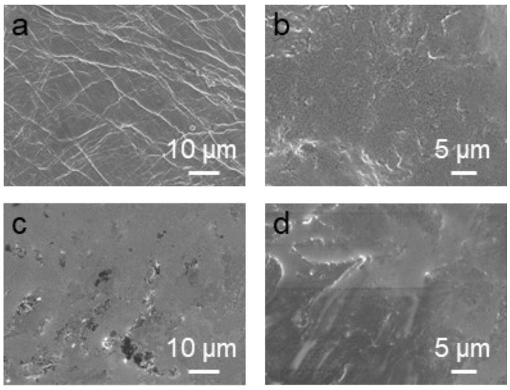

Figure S13. SEM images of metallic lithium anodes after cycling (a-b) at 0.05 mA cm^{-2} for 1500 h and (c-d) at 0.2 mA cm^{-2} for 500 h at room temperature.

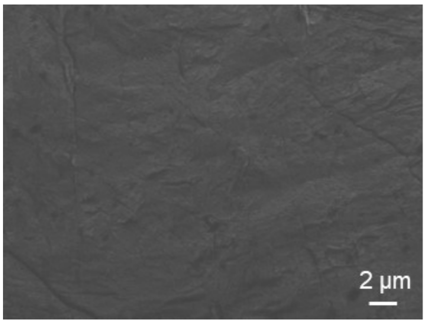

Figure S14. SEM images of the surface for metallic lithium anode with v-NBR/TAC/IL electrolyte after cycling at various current densities from 0.05 to 1 mA cm^{-2} at 0.05 mAh cm^{-2} at room temperature.

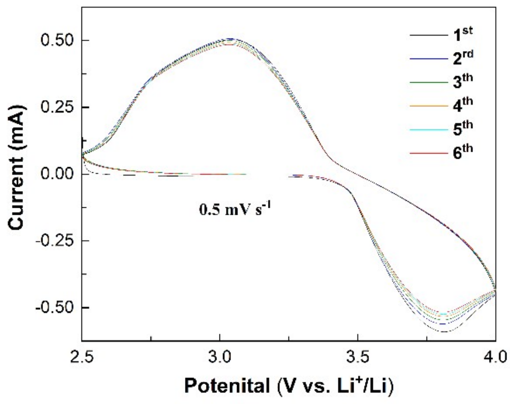

Figure S15. CV curves of Li-$LiFePO_4$ full battery with v-NBR/TAC/IL electrolyte at a scan rate of 0.5 mV s^{-1} at room temperature.

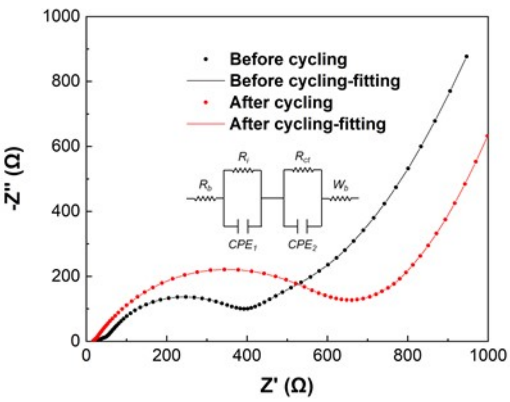

Figure S16. EIS plot of Li-$LiFePO_4$ full battery of v-NBR/TAC/IL before and after cycling at 0.5 C.

Table S1. Basic properties of flame retardant SPEs in this work compared with others

Electrolyte	Thickness (μm)	Ionic conductivity (S cm^{-1})	Mechanical strength (MPa)	Reference
PI/DBDPE/PEO/LiTFSI	10~65	6.7×10^{-6} (30 °C)	440	1
PEGBCDMA	-	$\sim10^{-6}$	0.24	2
Polyphosphoester copolymers	-	2×10^{-4} (70 °C)	-	3
ADP/PEO/LiTFSI	~100	3.7×10^{-5} (30 °C)	-	4
PI/PEO/LiTFSI	8.6	1.4×10^{-4} (25 °C)	-	5
Poly-DOL	~25	0.98×10^{-4} (30 °C)	-	6
SHSPE3	-	$\sim5\times10^{-5}$ (60 °C)	-	7
PGPE-4000	-	5.85×10^{-5} (RT)	-	8
FR-PU-20% Li	-	1.51×10^{-4} (70 °C)	1.26	9
v-NBR/TAC	~65	9.6×10^{-7} (RT)	0.68	This work
v-NBR/TAC/IL	~65	2.2×10^{-4} (RT)	0.52	This work

Reference.

1. Y. Cui, J. Wan, Y. Ye, K. Liu, L. Y. Chou and Y. Cui, *Nano Lett.*, 2020, **20**, 1686-1692.
2. G. Fu, M. D. Soucek and T. Kyu, *Solid State Ionics*, 2018, **320**, 310-315.
3. J. L. Olmedo-Martínez, L. Meabe, R. Riva, G. Guzmán-González, L. Porcarelli, M. Forsyth, A. Mugica, I. Calafel, A. J. Müller, P. Lecomte, C. Jérôme and D. Mecerreyes, *Polym. Chem.*, 2021, **12**, 3441-3450.
4. L. Han, C. Liao, X. Mu, N. Wu, Z. Xu, J. Wang, L. Song, Y. Kan and Y. Hu, *Nano Lett.*, 2021, **21**, 4447-4453.
5. J. Wan, J. Xie, X. Kong, Z. Liu, K. Liu, F. Shi, A. Pei, H. Chen, W. Chen, J. Chen, X. Zhang, L. Zong, J. Wang, L. Q. Chen, J. Qin and Y. Cui, *Nat. Nanotechnol.*, 2019, **14**, 705-711.
6. J. Xiang, Y. Zhang, B. Zhang, L. Yuan, X. Liu, Z. Cheng, Y. Yang, X. Zhang, Z. Li, Y. Shen, J. Jiang and Y. Huang, *Energy Environ. Sci.*, 2021, **14**, 3510-3521.
7. C. Wang, R. Li, P. Chen, Y. Fu, X. Ma, T. Shen, B. Zhou, K. Chen, J. Fu, X. Bao, W. Yan and Y. Yang, *J. Mater. Chem. A*, 2021, **9**, 4758-4769.
8. X. Zhang, C. Wang, W. Zhao, M. Han, J. Sun and Q. Wang, *Eur. Polym. J*, 2022, **176**, 111400-111409.
9. J. Chen, Z. Liu, J. Liu, X. Liu, X. Yang and X. Jiang, *Mater. Chem. Phys.*, 2022, **279**.